7th Annual International IEEE EMBS Conference on Neural Engineering
Montpellier, France, 22 - 24 April, 2015

Modeling the Effects of Electrode Recessing on Electrochemical Safety in Cochlear Implant Electrodes

Andrian Sue, *Student Member*, *IEEE*, Paul Wong, Phillip Tran, Qing Li, and Paul Carter

***Abstract*— Electrodes in neural prostheses may trigger stimulation-induced tissue damage if the magnitude of the stimulation exceeds safe levels. Consequently, the concentration of current densities at the periphery of planar electrodes has been studied extensively, and the use of electrode recesses has been suggested as a method of reducing such effects. Cochlear implant electrodes have significant geometrical differences from the planar electrodes used in earlier studies. We have previously used the finite element method to solve for current distributions on half-band cochlear implant electrodes. In this paper, we utilize similar models to investigate the effect of recessing half-band cochlear implant electrodes on their electrochemical safety. It was found that when recess depths were increased, the distribution of the electrodes became more uniform by up to 75.5%. The maximum reduction in irreversible faradaic reactions was found to be only 6.5% at the maximum recess depth, however other factors may contribute to the occurrence of irreversible faradaic reactions.**

I. INTRODUCTION

The geometry of electrodes used in neural prostheses varies according to the application. The platinum electrodes of a cochlear implant (CI) conform to a cylindrical silicone carrier due to the geometrical constraints of the scala tympani. Recent CI electrodes have adopted a half-band geometry to direct the charge towards the modiolus and the auditory nerve fibers, with the aim of increasing current localization in the cochlea [1]. These electrodes differ in both application and geometry from the planar electrodes used in important studies of electrode safety found in the literature [2]–[4].

Analytical models of planar electrodes emphasized the importance of current concentration at the edges in the context of neural stimulation [5], [6]. These current concentrations, known as "edge effects", have implications on the safety of stimulation, as localized peaks in charge density may drive irreversible processes at the electrode, including platinum dissolution, hydrogen (H_2) and oxygen (O_2) gas evolution and the oxidation of organic compounds [7]. Tissue damage may also occur by "mass action" inducing excitotoxicity in the excitable tissues if the charge delivered is beyond safe limits [4], [8], [9]. Previous works have shown that current concentrates at high curvature regions of electrode geometries, such as the crests of high perimeter electrodes [10], tips of needle electrodes [11], and the vertices of CI-like half-band electrodes [12]. Early models suggested recessing the electrode to eliminate the non-uniform current distribution on the electrode surface [5], [6], based on studies of planar disc electrodes. Rubinstein *et al.* [5] found a recess depth one-third of the radius provided relatively uniform distribution, without exceeding particular electrode design constraints. Some CI electrodes are slightly recessed into the silicone carrier to ensure their mechanical stability. Recess depths vary in the range of 10-100 μm depending on the position of the electrode on the array, but are constant across a single electrode pad. The influence of recess depth on the electrochemical safety of non-planar CI electrodes is unclear.

Most computational models of CIs have focused primarily on the current density and field distributions in the cochlea, enabling the analysis of neural excitation and the calculation of impedances [13]–[16]. These models have ignored or provided relatively simple representations of the electrode-electrolyte interface. Recent studies have effectively utilized the finite element (FE) method to model the current density distributions at the electrode-tissue interface in the broader context of electrode safety [11], [12], [17], but with simplified electrode geometries. This study aims to use the FE method to model half-band CI electrodes at various recess depths, and analyze their effect on the levels of irreversible faradaic reactions.

II. METHODS

Greater detail of the modeling used in this paper has been previously documented [12]. The methodology is briefly outlined here, with changes relevant to the current study.

A. Geometry

The model geometries were constructed in the FE software, COMSOL v4.4 (COMSOL AB, Stockholm, Sweden). The geometry consisted of a single platinum half-band electrode (σ = 94×10^5 S/m, ε = 1), associated silicone cylindrical carrier ($\sigma = 1\times10^{-14}$ S/m, $\varepsilon = 4$), and surrounding cylindrical saline testing chamber (σ = 1.4 S/m, ε = 80), as seen in Fig. 1. The diameter and length of the testing chamber were 2 mm and 0.85 mm respectively, to mimic the dimensions of the scala tympani and a Nucleus straight electrode array. The half-band width (HBW in Fig. 1) was 300 μm and constant electrode recess depths (RD in Fig. 1) of 10 μm to 100 μm were applied to each electrode by increasing the thickness of the silicone carrier.

Research supported by the Australian Research Council (ARC) and Cochlear Ltd. A. Sue, P. Tran & P. Wong are recipients of Australian Postgraduate Awards (APAs).

All authors are with the School of Aerospace, Mechanical and Mechatronic Engineering, Faculty of Engineering and IT, University of Sydney, NSW 2006 Australia. (Tel.: +612-9351-5674; Fax: +612-9351-7060; email: andrian.sue@sydney.edu.au, qing.li@sydney.edu.au)

P. Carter is also a Technology Cluster Leader with Cochlear Ltd., Macquarie University, NSW 2109 Australia. (email: pcarter@cochlear.com)

978-1-4673-6389-1/15/$31.00 ©2015 IEEE

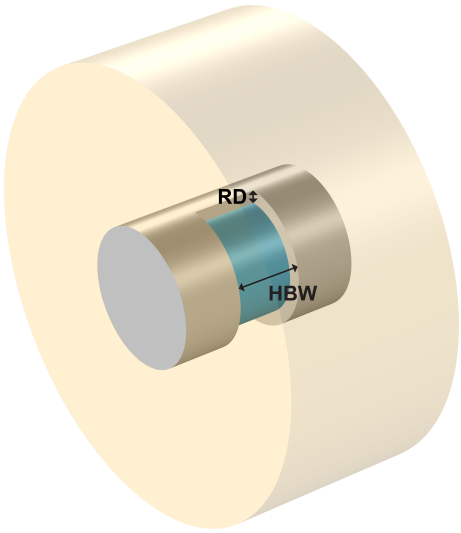

Fig. 1. Model geometry showing a recessed half-band electrode (blue) with surrounding silicone carrier (grey). The recess depth (RD) and half-band width (HBW) are varied to study their effects on the electrochemical behavior of the electrode under constant charge density conditions. The saline test chamber (yellow) surrounds the electrode.

TABLE I
DESCRIPTION AND VALUES FOR PARAMETERS USED IN (2)

Description	Parameter	Value
Anodic Transfer Coefficient	α_a	0.29
Cathodic Transfer Coefficient	α_c	0.23
Exchange Current Density	i_0	1×10^{-6} A/m^2
Electrons	n	2
Temperature	T	298 K

B. Boundary Conditions

Electrical grounds were applied as Dirichlet boundary conditions ($V = 0$) to both ends of the saline testing chamber. A constant current stimulus was fed to the electrode by assigning a current terminal to its inside surface. All other surfaces of the model, and the surfaces between the electrode and carrier, were electrically insulated ($\mathbf{n} \cdot \mathbf{J} = 0$).

The electrochemical behavior of the platinum electrode was modeled using an electrical impedance boundary condition on the electrode surface. The total impedance of the boundary accounted for both reversible non-faradaic and irreversible faradaic processes. A constant-phase model, defined in (1) was adopted to model the non-faradaic processes. An inverse Laplace transformation was used to translate this frequency-dependent impedance into the time-domain. This technique has been discussed previously [12], [18]. In (1), the constant phase coefficient (K) and exponent (β) are empirically-determined, and constant values were used consistent with other sophisticated electrode models [11], [19].

$$Z_{CPA} = K(i\omega)^{-\beta} \tag{1}$$

$$Z_{CT} = \frac{\eta}{i_0 \{e^{-\alpha_c n f \eta} - e^{\alpha_a n f \eta}\}} \tag{2}$$

Faradaic reactions were assumed to be non-linear and totally irreversible. The Butler-Volmer equation (2) was used to model this behavior in the form of a charge transfer impedance (Z_{CT}). The parameters in (2) were estimated for oxygen (O_2) and hydrogen (H_2) from published cyclic voltammetry data for platinum electrodes in oxygen-deficient buffered saline [20]. Values for these parameters and their descriptions are provided in Table I.

C. Solution

Geometries were meshed into second-order tetrahedral elements, with increasing density closest to the electrode surface. The minimum number of nodes on the electrode surface was 33884. The models were computed in COMSOL using the MUMPS direct linear solver coupled to a non-linear damped Newton solver. Time-stepping was performed for the duration of the pulse width, in this case, 75 μs. The current provided to the electrode was set according to the geometric electrode area and a charge density of 16 μC/cm^2/phase.

III. RESULTS

The FE models enabled the separation of the non-faradaic and irreversible faradaic components of the delivered electrical current. The irreversible faradaic current density (J_{CT}) distributions are shown in Fig. 2 for electrodes with varying RD. The maximum J_{CT} on the electrode surface was found to be at the corners of the half-band electrode. Larger RDs reduced the peak values of J_{CT}, representing a decrease in the amount of gas evolution occurring at these corners. The minimum values also increased slightly as a result of this reduction. Overall, the magnification of J_{CT} at the corners, although not totally eliminated at the maximum RD of 100 μm, were effectively controlled by recessing the electrode.

Normalizing the maximum J_{CT} against the minimum J_{CT} provided a "distribution ratio" indicative of the non-uniformity of the irreversible faradaic reactions on the electrode surface (Fig. 3(a)). The percentage reduction in the distribution ratio between 20 μm and 40 μm was 36.1%, which indicated a large reduction in non-uniformity with a small change in RD. When RDs were larger, these improvements were diminished, with a smaller reduction of 12.7% from 80 μm to 100 μm. The total percentage reduction from 10 μm to 100 μm was 75.5%.

The magnitude of irreversible faradaic reactions occurring on the electrode surface was recorded as the associated current, I_{CT} at the end of the current pulse. This measure is representative of the total charge consumed by the modeled irreversible faradaic reaction [12]. I_{CT} decreased with increasing RD (Fig. 3(b)), similar to the distribution ratio in Fig. 3(a). The magnitude of the decrease was 0.91 nA (6.5%) between the maximum and minimum RDs.

IV. DISCUSSION

Recessed electrodes have been explored as a way to reduce edge effects, which have a negative impact in many bioelectric applications [5], [6], [21]–[23]. Existing electrode models are commonly two-dimensional and make quasi-static

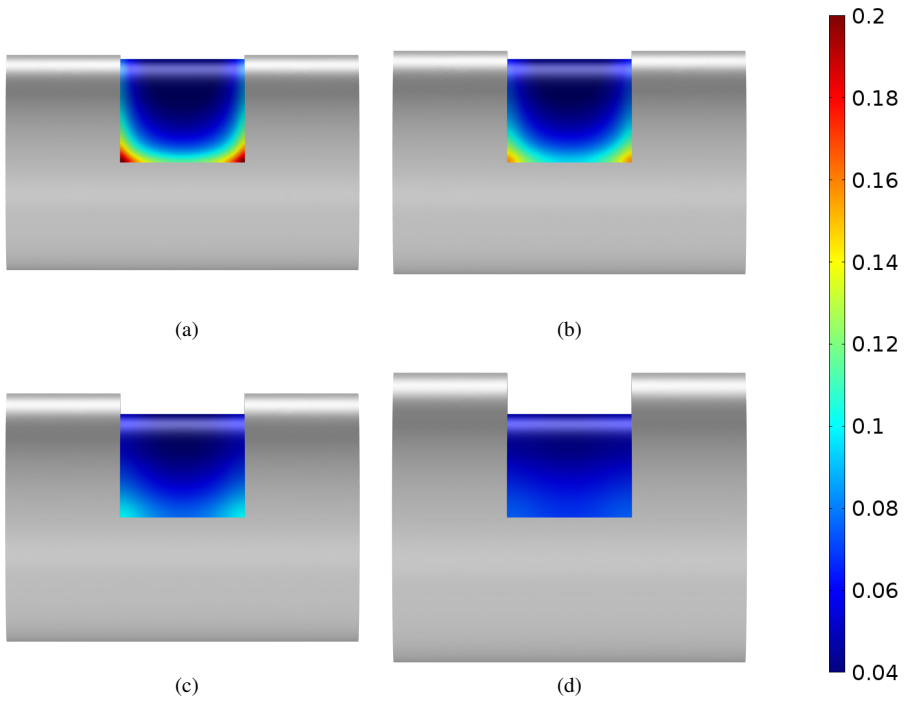

Fig. 2. Side view of the half-band electrode showing J_{CT} distributions on the exposed electrode surface. Results for recess depths of (a) 10 μm, (b) 20 μm, (c) 50 μm, and (d) 100 μm are plotted in A/m^2. Maximum J_{CT} values are 0.210 A/m^2, 0.156 A/m^2, 0.100 A/m^2, and 0.075 A/m^2 for plots (a)-(d), respectively. Maximum J_{CT} was consistently located at the corners of the half-band electrodes.

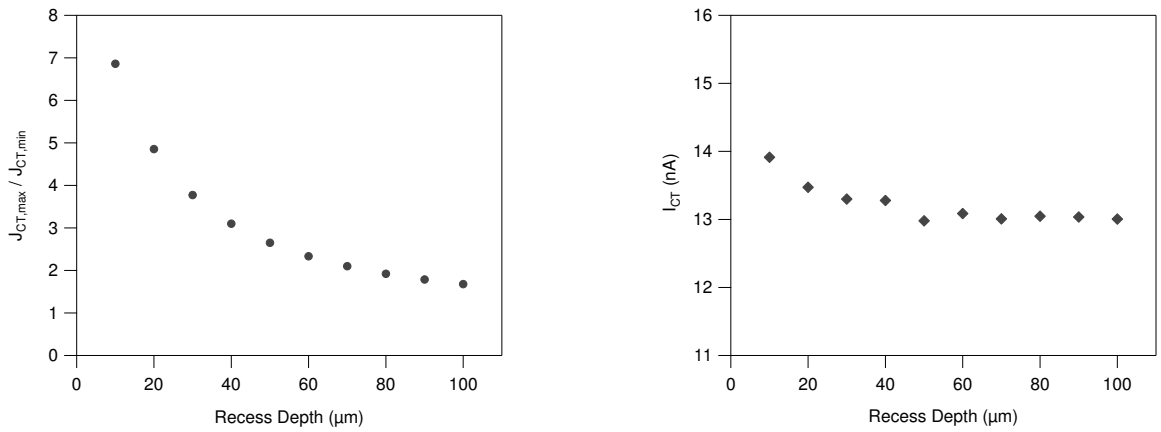

Fig. 3. Measurements of irreversible faradaic activity for electrodes of varying RD. (a) shows the ratio of the maximum ($J_{CT,max}$) to the minimum ($J_{CT,min}$) faradaic current densities at the end of the current pulse (t = 75 μs), and (b) shows the instantaneous current (I_{CT}) flowing through the irreversible gas evolution pathway at the end of the current pulse.

assumptions regarding the electrode current density distributions. In this paper, we have presented three-dimensional models of recessed half-band CI electrodes, encompassing the kinetics of irreversible gas evolution, which can be used to define unsafe charge injection, and therefore, safe charge injection limits [9], [24].

The J_{CT} distributions on the electrode surface exhibit similarities to those for planar disc electrodes calculated by Rubinstein *et al.* [5], showing diminished improvement, measured as reduction in current density non-uniformity with increasing recess depth. The effect of the boundary conditions and the presence of corners in the electrode geometry should also be considered. This is reflected in non-uniformity of current densities along the perimeter of the electrode shown in Fig. 2. The geometry of the testing chamber forces current to spread along the axis of the cylindrical domain towards the applied Dirichlet boundary conditions, intensifying the concentration of J_{CT} on the electrode corners. Therefore, the behavior of the electrodes *in vivo* should be functions of the surrounding cochlea geometry

and the location of the counter electrodes. These factors result in different responses to recess depth observed for half-band CI electrodes when compared to planar electrodes.

While the reduction of edge effects with recess depth are easily observed, changes to the total levels of irreversible gas evolution (I_{CT}) are less obvious. Earlier studies used "high" local current densities as a measure of stimulation-induced tissue injury, but were not able to evaluate the electrochemical reactions that may contribute to damage [5]. The reductions in I_{CT} in Fig. 3(b) are more modest than those implied from the aforementioned models. This suggests that creating highly recessed electrodes will not provide the anticipated improvements to electrochemical charge injection limits. Future modeling studies will seek to further investigate the influence of electrode geometry, including shape and depth of recesses over electrodes [6], [22], on the electrochemical safety of CI stimulation.

Modeling assumptions were made in this study to simplify the evaluation of the electrodes. Only cathodic phases were simulated as this was adequate for a comparison of the effects of recess depth. The presence of residual direct currents resulting from biphasic stimulation has been associated with tissue injury [25], and warrants further study of biphasic pulses using similar FE models. The application of the Butler-Volmer equation assumes that the electrode current flow is limited by electron transfer kinetics at the electrode-electrolyte interface, thus ignoring the effect of the concentrations of the products and reactants near the electrode [26]. Reversible faradaic reactions were considered pseudocapacitive in nature and contribute to the constant-phase behavior described in the model [19], [24]. Improvements to the existing model may involve the inclusion of diffusion kinetics to accurately simulate reversible processes.

V. CONCLUSIONS

The FE models described in this paper were successfully used to investigate the impact of electrode recessing on the electrochemistry of half-band CI electrodes. Results from the models show that recessing decreased the extent of gas evolution on the electrodes but by much less than that suggested by previous quasi-static models. Future work will aim to increase the sophistication of the electrochemical model and explore CI electrode design parameters that can influence safe charge injection.

REFERENCES

[1] M. Tykocinski, E. Saunders, L. T. Cohen, C. Treaba, R. J. Briggs, P. Gibson, G. M. Clark, and R. S. Cowan, "The contour electrode array: safety study and initial patient trials of a new perimodiolar design," *Otology & Neurotology*, vol. 22, no. 1, pp. 33–41, 2000.

[2] D. B. McCreery, W. F. Agnew, T. G. H. Yuen, and L. A. Bullara, "Comparison of neural damage induced by electrical stimulation with faradaic and capacitor electrodes.," *Annals of Biomedical Engineering*, vol. 16, no. 5, pp. 463–481, 1988.

[3] D. B. McCreery, W. F. Agnew, T. G. H. Yuen, and L. A. Bullara, "Charge density and charge per phase as cofactors in neural injury induced by electrical stimulation," *IEEE Transactions on Biomedical Engineering*, vol. 37, no. 10, pp. 996–1001, 1990.

[4] R. V. Shannon, "A model of safe levels for electrical stimulation," *IEEE Transactions on Biomedical Engineering*, vol. 39, no. 4, pp. 424–426, 1992.

[5] J. T. Rubinstein, F. A. Spelman, M. Soma, and M. F. Suesserman, "Current density profiles of surface mounted and recessed electrodes for neural prostheses," *IEEE Transactions on Biomedical Engineering*, no. 11, pp. 864–875, 1987.

[6] M. F. Suesserman, F. A. Spelman, and J. T. Rubinstein, "In vitro measurement and characterization of current density profiles produced by non-recessed, simple recessed, and radially varying recessed stimulating electrodes.," *IEEE Transactions on Biomedical Engineering*, vol. 38, no. 5, pp. 401–408, May 1991.

[7] S. B. Brummer and M. J. Turner, "Electrochemical Considerations for Safe Electrical Stimulation of the Nervous System with Platinum Electrodes," *IEEE Transactions on Biomedical Engineering*, vol. 24, no. 1, pp. 59–63, 1977.

[8] W. F. Agnew and D. B. McCreery, "Considerations for safety with chronically implanted nerve electrodes.," *Epilepsia*, vol. 31, pp. S27–32, 1990.

[9] D. R. Merrill, M. Bikson, and J. G. R. Jefferys, "Electrical stimulation of excitable tissue: design of efficacious and safe protocols.," *Journal of Neuroscience Methods*, vol. 141, no. 2, pp. 171–198, Feb. 2005.

[10] X. F. Wei and W. M. Grill, "Analysis of high-perimeter planar electrodes for efficient neural stimulation.," *Frontiers in Neuroengineering*, vol. 2, p. 15, 2009.

[11] D. R. Cantrell, S. Inayat, A. Taflove, R. S. Ruoff, and J. B. Troy, "Incorporation of the electrode-electrolyte interface into finite-element models of metal microelectrodes," *Journal of Neural Engineering*, vol. 5, no. 1, pp. 54–67, 2008.

[12] A. Sue, P. Tran, P. Wong, Q. Li, and P. M. Carter, "Time-domain finite element models of electrochemistry in intracochlear electrodes," presented at the *2013 35th Annual International Conference of the IEEE Engineering in Medicine and Biology Society (EMBC)*, 2013, pp. 1554–1557.

[13] J. J. Briaire and J. H. M. Frijns, "Field patterns in a 3D tapered spiral model of the electrically stimulated cochlea.," *Hearing Research*, vol. 148, no. 1, pp. 18–30, Oct. 2000.

[14] T. Hanekom, "Three-dimensional spiraling finite element model of the electrically stimulated cochlea.," *Ear and Hearing*, vol. 22, no. 4, pp. 300–315, Aug. 2001.

[15] F. J. Vanpoucke, A. J. Zarowski, and S. A. Peeters, "Identification of the impedance model of an implanted cochlear prosthesis from intracochlear potential measurements," *IEEE Transactions on Biomedical Engineering*, vol. 51, no. 12, pp. 2174–2183, 2004.

[16] W.-D. Lai and C. T. M. Choi, "Incorporating the Electrode-Tissue Interface to Cochlear Implant Models," *IEEE Transactions on Magnetics*, vol. 43, no. 4, pp. 1721–1724, Apr. 2007.

[17] M. R. Behrend, A. K. Ahuja, and J. D. Weiland, "Dynamic Current Density of the Disk Electrode Double-Layer," *IEEE Transactions on Biomedical Engineering*, vol. 55, no. 3, pp. 1056–1062, Mar. 2008.

[18] A. Sadkowski, "Time domain responses of constant phase electrodes," *Electrochimica Acta*, vol. 38, no. 14, pp. 2051–2054, 1993.

[19] A. Richardot and E. T. McAdams, "Harmonic analysis of low-frequency bioelectrode behavior," *IEEE Transactions on Medical Imaging*, vol. 21, no. 6, pp. 604–612, Jun. 2002.

[20] E. M. Hudak, J. T. Mortimer, and H. B. Martin, "Platinum for neural stimulation: voltammetry considerations," *Journal of Neural Engineering*, vol. 7, no. 2, p. 026005, 2010.

[21] S. Tungjitkusolmun, E. J. Woo, H. Cao, J. Z. Tsai, V. R. Vorperian, and J. G. Webster, "Finite element analyses of uniform current density electrodes for radio-frequency cardiac ablation," *IEEE Transactions on Biomedical Engineering*, vol. 47, no. 1, pp. 32–40, 2000.

[22] Y. Song, E. Lee, E. J. Woo, and J. K. Seo, "Optimal geometry toward uniform current density electrodes," *Inverse Problems*, vol. 27, no. 7, p. 075004, 2011.

[23] E. K. Brunton, A. J. Lowery, and R. Rajan, "A comparison of microelectrodes for a visual cortical prosthesis using finite element analysis," *Frontiers in Neuroengineering*, vol. 5, no. 23, 2012.

[24] S. F. Cogan, "Neural Stimulation and Recording Electrodes," *Annual Review of Biomedical Engineering*, vol. 10, no. 1, pp. 275–309, 2008.

[25] C. Q. Huang, R. K. Shepherd, P. M. Carter, P. M. Seligman, and B. Tabor, "Electrical stimulation of the auditory nerve: direct current measurement in vivo," *IEEE Transactions on Biomedical Engineering*, vol. 46, no. 4, pp. 461–469, 1999.

[26] A. J. Bard and L. R. Faulkner, Electrochemical Methods: Fundamentals and Applications, 2nd ed. New York, NY: John Wiley & Sons, 2001.